Title:
Trochoidal Pocket Machining with Tool Engagement Control

Authors:
Martin Held, held@cs.sbg.ac.at, Universität Salzburg
Josef Pfeiffer, jpfeiffer@cs.sbg.ac.at, Universität Salzburg

Keywords:
Pocket Machining, Engagement Angle, Trochoidal Path, MATHSM, Voronoi Diagram

DOI: 10.14733/cadconfP.2024.158-163

Introduction:
Virtually all CAD/CAM software offer options for generating tool paths for pocket machining. However, while these paths can be expected to be correct from a purely geometric point of view, they do not necessarily take into account key process parameters like the cutting width and the tool engagement angle. The *radial width of cut*, υ, frequently simply called *cutting width*, is commonly defined as the radial amount of the tool that is engaged in the material; see Fig. 1a. However, the actual immersion depth δ may be substantially larger than υ. Hence, the actual cutting forces are better reflected by the *tool engagement angle* θ: It is the angle subtended by the circular arc that corresponds to the contact surface of the tool disk with the material being machined. (In Fig. 1, this arc is shown in dashed green.)

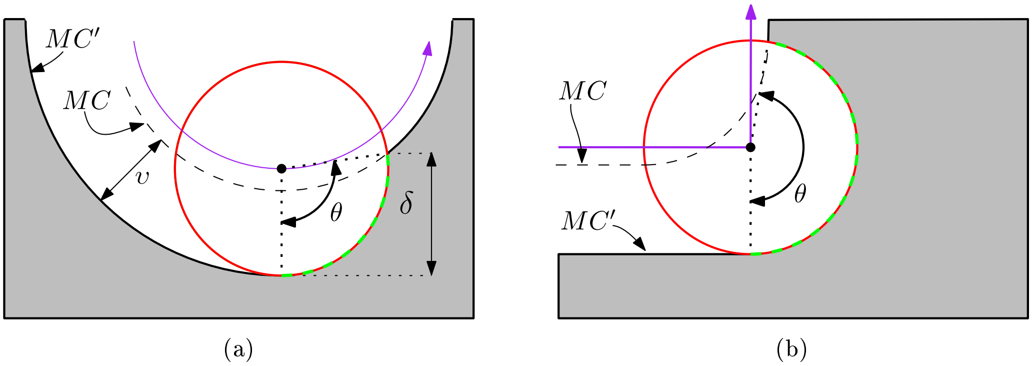

Fig. 1: Cutting width υ and engagement angle θ for the motion of a tool (depicted by a red disk) along a tool path (shown in purple). The old machining contour is denoted by MC and the new contour is denoted by MC'. The unmachined material is shaded grey.

Our Contribution:
Little is known on global strategies to generate tool paths for pocketing such that a user-specified maximum engagement angle is not exceeded. Most pocketing papers either ignore the engagement angle

Proceedings of CAD'24, Eger, Hungary, July 1-3, 2024, 158-163
© 2024 U-turn Press LLC, http://www.cad-conference.net

completely or provide only heuristics. We provide an extension of the (one-sided) MATHSM pocketing strategy by Elber, Cohen and Drake [1] for pockets bounded by straight-line segments and circular arcs. Rather than blindly resorting to some fixed constant step-over distance, we adapt the step-over distance between each pair of subsequent circular path segments such that the tool engagement angle reaches but never exceeds a user-specified limit. As a more global optimization we keep track of the area already machined. This allows to increase the step-over distance even further if previous machining operations in other parts of the pocket have already covered some portion of the material that is currently to be removed. By analyzing the pocket geometry we are able to dynamically adapt the limit on the engagement angle depending on the "narrowness" of parts of the pocket. (These improvements of our standard algorithm are not discussed in this extended abstract, though.) Experiments show that our improvements tend to result in substantially shorter tool paths compared to our implementation of the original MATHSM method, while guaranteeing that the engagement angle does not exceed the user-specified limit.

Tool Path Computation:

We study tool paths for pockets $\mathcal{P}$ (without holes) bounded by straight-line segments and circular arcs. The pocket boundary $\partial\mathcal{P}$ is assumed to be one Jordan curve that is oriented counter-clockwise (CCW). This orientation imposes an orientation of the straight-line segments and circular arcs of the boundary in a natural way. We call a circular arc *concave* if it is oriented clockwise (CW), and *convex* otherwise. We assume that the radii of all convex arcs are greater than the radius r of the tool. (Otherwise the pocket cannot be machined completely with that tool without gouging.) Our tool paths are suitable for conventional milling. It would be straightforward to modify our approach such that climb milling is supported.

As usual, a disk centered at a point p within (the closure of) $\mathcal{P}$ is called a *clearance disk* if the entire disk is completely contained inside (the closure of) $\mathcal{P}$ and if its radius cannot be enlarged without protruding outside of $\mathcal{P}$. The radius of the clearance disk of a point p is called the *clearance distance* of p. Roughly, the medial axis of $\partial\mathcal{P}$ (within $\mathcal{P}$) is given by the union of the centers of all those clearance disks of $\mathcal{P}$ which touch $\partial\mathcal{P}$ in at least two disjoint points. The medial axis is a subset of the Voronoi diagram of $\partial\mathcal{P}$, and it can be derived easily from the Voronoi diagram. We refer to Held [2] for a detailed discussion of Voronoi diagrams, medial axes and their use for offsetting. Our own implementation relies on Voronoi diagrams and medial axes computed by means of VRONI/ARCVRONI [3].

Consider a point c_{i-1} with clearance disk A_{i-1} and clearance distance $\rho_{i-1}+r$ within $\mathcal{P}$ (for $\rho_{i-1} > 0$). The circle M_{i-1} centered at c_{i-1} with radius ρ_{i-1} is the *machining circle* of c_{i-1}, and c_{i-1} is its *machining center*. Similarly for some other machining center c_i and its machining circle M_i; cf. Fig. 2. These machining circles are the main curves used by the MATHSM algorithm by Elber, Cohen and Drake [1] to move the tool disk. In order to end up with one continuous path, two subsequent machining circles M_{i-1} and M_i are linked by a *transition element* T_{i-1} as follows: The offset curve for offset distance r is intersected with the line segment between c_{i-1} and p_{i-1}, yielding a point q_{i-1}. Similarly we get q_i as the intersection of the line segment between c_i and p_i with the offset curve. Then T_{i-1} is obtained by moving along the offset curve from p_{i-1} to p_i in CCW manner. This construction yields the following part of a trochoidal tool path: The center of the tool starts at q_{i-1}, moves along M_{i-1} once in CCW direction until it returns to q_{i-1}, and then proceeds along the transition element T_{i-1} to q_i. From there it would continue CCW along M_i, etc.

It is obvious that a distant spacing of the machining circles as shown in Fig. 2 would not be suitable for a real machining process. For the one-sided MATHSM, Elber et al. [1] place a machining center c_i such that it is the midpoint of q_i and the (closest) intersection point m_i of the medial axis of $\mathcal{P}$ with the line through p_i and c_i. Thus, the line segment between m_i and q_i forms a diameter of M_i with center c_i; see Fig. 2. The actual spacing of the machining centers is not discussed in [1]. However, comments in

© 2024 U-turn Press LLC, http://www.cad-conference.net

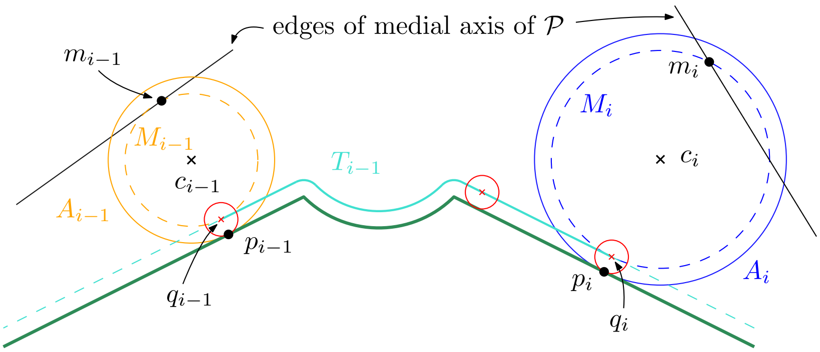

Fig. 2: The basic building blocks of a MATHSM path: Two subsequent machining circles M_{i-1} and M_i and the transition element T_{i-1} (in turquoise) for linking them. The pocket boundary $\partial\mathcal{P}$ is indicated by a dark green line and its offset curve (for offset distance r) is drawn as a dashed turquoise line. The three small red circles depict the tool disk.

its section on extending the basic MATHSM algorithm suggest that some (unknown) constant spacing is applied, either with $\|c_i - c_{i-1}\|$ or with $\|m_i - m_{i-1}\|$ being constant. In the end of their paper, they comment that a dynamic strategy that adapts the spacing distances according to machining parameters can be expected to be beneficial. We pick up this lead and extend their MATHSM algorithm such that a spacing of the machining centers is obtained that keeps the tool engagement angle below a user-specified limit.

Computing the Engagement Angle:

Suppose that the tool with radius r has moved along the machining circle M_{i-1} with radius ρ_{i-1} centered at c_{i-1}, and suppose that all material within the circle A_{i-1} has been removed. Let q be a position of the tool center on M_i for which cutting occurs. We denote the intersections of the tool circle with A_{i-1} by a and b, with b being that point the tool has not yet swept over, cf. Fig. 3a. The intersection point of the ray from c_i through q with A_i is denoted by w. Then the engagement angle of the tool centered at q is given by the angle $\theta := \angle bqw$ at the vertex q of the triangle $\Delta(b, q, w)$. We note that fixing the position of q on M_i also fixes the position of b on A_{i-1}, and vice versa.

For which position q of the tool center on M_i is θ maximized? Trivially, maximizing θ is equivalent to minimizing the angle $\angle c_i qb$ at the vertex q of the triangle $\Delta(c_i, q, b)$. By construction, we have $\|q - c_i\| = \rho_i$ and $\|q - b\| = r$. That is, these two edges of $\Delta(c_i, q, b)$ have fixed constant lengths. We conclude that the angle $\angle c_i qb$ is minimum exactly if the edge length $\|b - c_i\|$ is as short as possible. This happens when the points c_{i-1}, c_i and b are collinear and occur in that order along the common line.

However, naïvely placing q on M_i such that c_{i-1}, c_i and b are collinear may lead to an overestimation of the maximum engagement angle that occurs while moving the tool along M_i: Figure 3c shows a setting where w ends up within A_{i-1}. Since the tool does not interact with the material at w, the angle $\angle bqw$ exceeds the true engagement angle for this tool position. Now recall that moving b away from the line through c_{i-1} and c_i (along A_{i-1}) causes the engagement angle to decrease. Hence, we move b in CCW direction along A_{i-1} just far enough to allow w to coincide with the intersection of A_{i-1} and A_i. This approach can be cast into explicit formulas for θ in dependence on the machining center c_i and radius ρ_i.

Determining the Next Feasible Position of a Machining Circle:

We are now ready to describe how the next machining center c_i is determined such that the maximum

© 2024 U-turn Press LLC, http://www.cad-conference.net

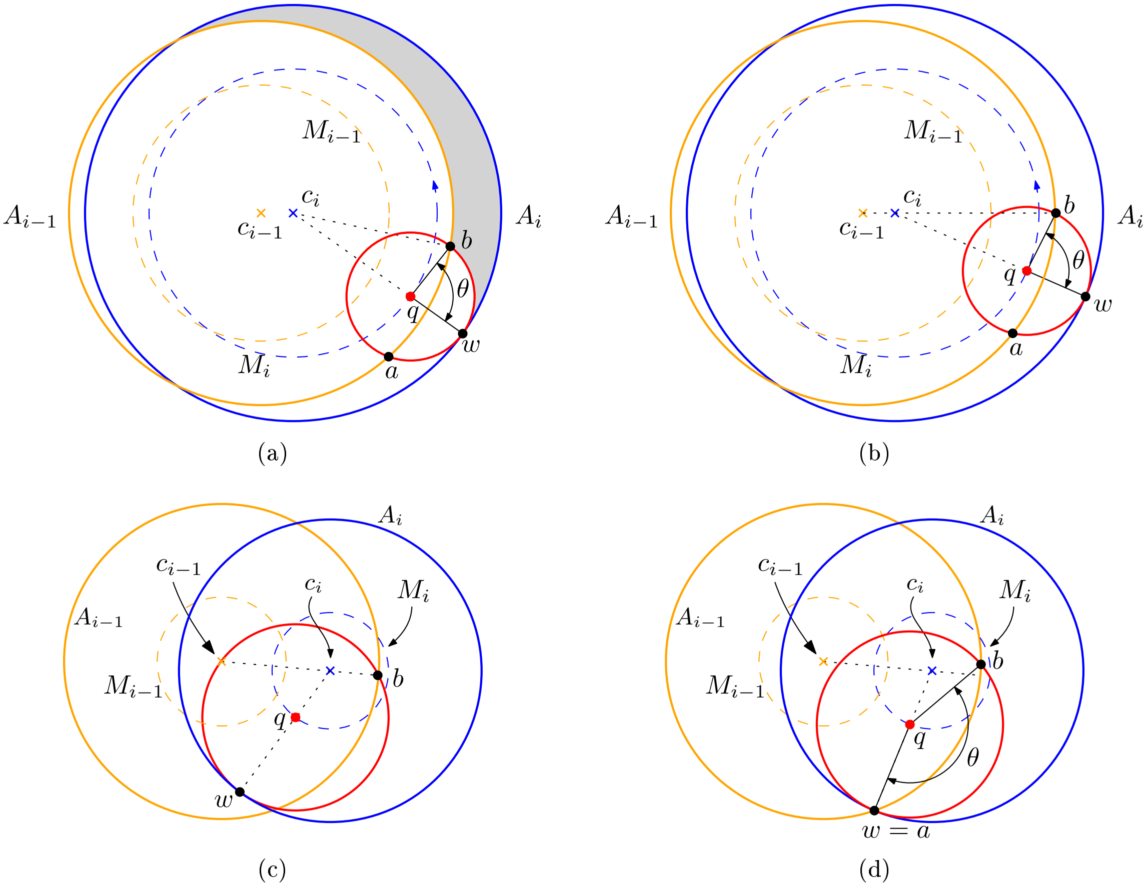

Fig. 3: Computing the maximum tool engagement angle when the (red) tool disk is moved CCW along the machining circle M_i. In (a) the setting is shown for a position q of the tool center; the engagement angle θ is given by the angle $\angle bqw$. The material yet to be removed is shaded grey. For the same geometric setting of M_{i-1} and M_i and the same tool radius, in (b) the tool position q for which the maximum engagement angle relative to A_{i-1} is assumed is shown. Subfigure (c) shows a setting for which the engagement angle would be overestimated if $\angle bqw$ would be considered because w lies within A_{i-1}. For this setting the correct maximum engagement angle is shown in (d).

engagement angle θ stays below a user-specified limit $\theta_{\max} < 180$. (If $\theta_{\max} := 180$ then full slotting moves were allowed and no tool path would exceed this limit.) No machining occurs if $\|c_i - c_{i-1}\| = 0$ and, thus, $\theta = 0$. The maximum engagement angle starts to grow as soon as c_i is moved away from c_{i-1} in the direction of the unmachined material. The explanation given in the previous section allows to compute the maximum engagement angle θ for any machining center c_i (relative to c_{i-1} and ρ_{i-1}). Unfortunately, we have not been able to find a closed-form solution for the inverse problem: Given $\theta_{\max}$, compute c_i such that moving the tool along M_i centered at c_i results in a maximum engagement angle $\theta = \theta_{\max}$.

As illustrated in Fig. 2, the MATHSM algorithm places c_i on a "middle" curve between the medial axis of $\mathcal{P}$ and $\partial\mathcal{P}$: The machining center c_i is at a distance ρ_i from the point m_i on the medial axis and at a distance $\rho_i + r$ from its normal projection p_i onto $\partial\mathcal{P}$. Standard mathematics implies a trivial upper

© 2024 U-turn Press LLC, http://www.cad-conference.net

bound on the maximum permissible distance d of c_i from c_{i-1}: We have $d < 2r + \rho_{i-1}$. If the distance d exceeds $2r + \rho_{i-1}$ then a full slotting move occurs and the engagement angle is guaranteed to be 180°.

Summarizing, for $d := 0$ we have $\theta = 0$ and for $d := 2r + \rho_{i-1}$ we have $\theta = 180$. Hence, we apply bisection to find a suitable spacing distance d between c_{i-1} and c_i such that $\theta = \theta_{\max}$. Experience drawn from myriads of invocations of the bisection routine tells us that the bisection needs 9–18 iterative steps to converge. Of course, we do not attempt to model the “middle” curve between the medial axis and $\partial\mathcal{P}$ explicitly as the loci of all potential machining centers. Rather, in parallel we move away from p_{i-1} along $\partial\mathcal{P}$ (in CCW direction) towards p_i and accordingly from m_{i-1} along the medial axis towards m_i. This traversing of the medial axis required for locating m_i is very similar to the traversing required for offsetting, and we refer to literature on Voronoi-based offsetting for details; see, e.g., [2].

Results Obtained:

We implemented our algorithm in C++. As already stated, Voronoi diagrams and medial axes are computed by means of Vroni/ArcVroni [3]. A constant spacing of the machining centers rather than a spacing based on the maximum engagement angle allows us to use our implementation to generate paths that mimic the original MATHSM algorithm.

In our experiments we studied the lengths of the tool paths and the distributions of the engagement angles along the paths. While summing the lengths of the individual straight-line segments and circular arcs suffices to compute the length of a path, assessing the engagement angles along a path requires a higher effort. For the sake of implementational simplicity, we compute the engagement angles for a myriad of densely spaced positions of the tool center along a path.

Since there is no apparent relation between the constant spacing d of the machining centers and the resulting maximum engagement angle for the MATHSM algorithm, we resorted to a brute-force solution: We varied the value d in tiny increments from small to large (relative to the tool radius and the geometry of a pocket), computed for every value of d the MATHSM path and recorded its maximum engagement angle (and its length).

This allowed us to compare our paths to the MATHSM paths such that all paths respect the same maximum engagement angle $\theta_{\max}$. In Fig. 4, sample paths are shown for $\theta_{\max} := 80$. In the figures, the start chosen for the tool path is depicted by a red tool circle and a red cross; it would be suitable for a spiral-down motion of the tool within a disk whose diameter matches roughly the tool diameter. Glancing at these two paths makes it immediately apparent that the path generated by our approach is substantially shorter than the MATHSM path that respects the same value of $\theta_{\max}$.

Figure 5 plots the engagement angles for hundreds of consecutive tool positions along the tool paths for our method and for the original MATHSM approach, for the setting of Fig. 4. For every position (of the center) of the tool a color-coded point indicates the engagement angle. No engagement angles were assessed during the spiral-down move within the white disk at the start of the path. We admit that the color coding is not entirely reliable in the close neighborhood of the edges of the medial axis due to multiple overlaps of the tool disk (which make it difficult to place the correctly colored point “on top” in the plots). Still, the plots make it evident why the original MATHSM paths are significantly longer than our paths: While our paths have engagement angles in the range 70° to 80° along large portions of the cutting moves, the MATHSM path has angles mostly in the range 30° to 60°. Only around the start of the path and in the very left region and very right region of the pocket the angles reach 80°. These regions enforce a small value for the spacing of the machining circles. As it can be seen, such a small spacing constitutes a waste for most portions of the path, thus leading to an excessively long path.

Of course, the results obtained depend on the geometry of the pocket and on the size of the tool. And they depend on the start of the tool path, too. Still, overall the results for other pockets, tool sizes and start points of the paths are similar to the results presented for the setting of Fig. 4.

© 2024 U-turn Press LLC, http://www.cad-conference.net

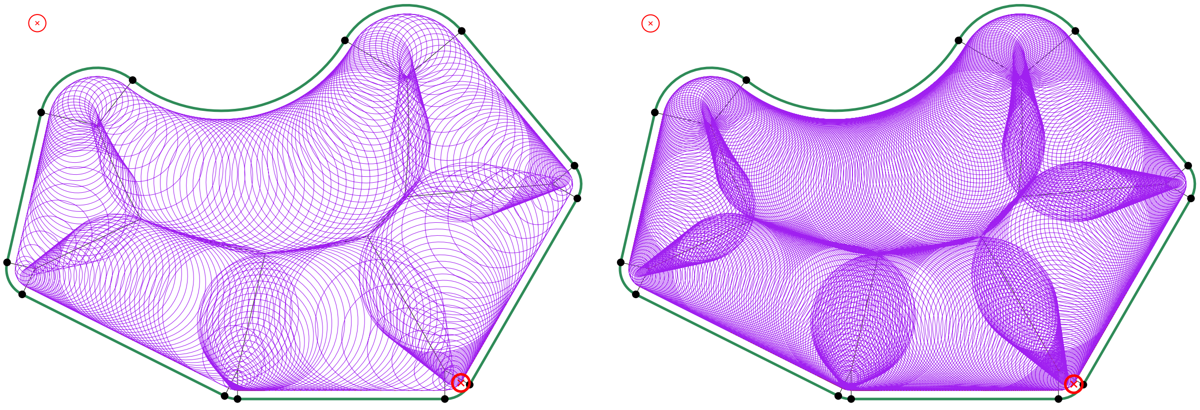

(a) (b)

Fig. 4: Sample tool paths for $\theta_{\max} := 80$ and the tool shown in the upper-left corners of the figures: The path in (a) was generated by our algorithm, while (b) shows the result for our implementation of the original MATHSM algorithm.

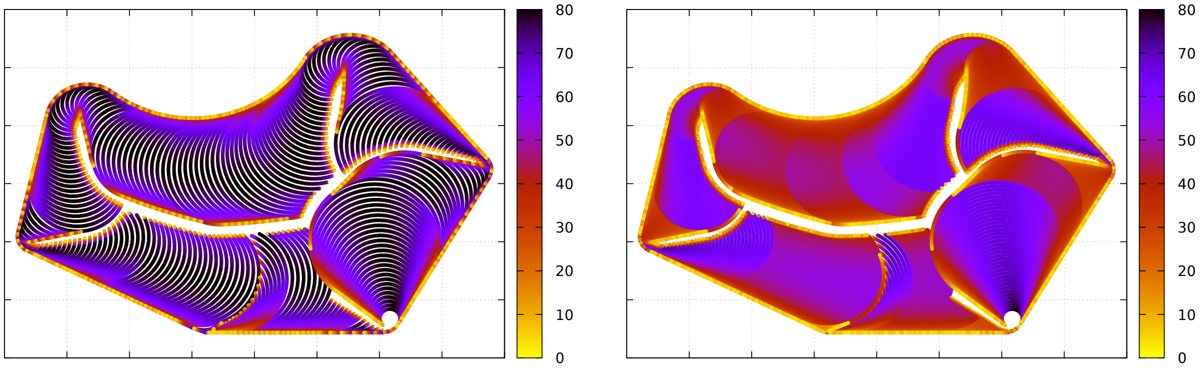

(a) (b)

Fig. 5: Plots that show the distribution of the engagement angles along the tool paths for our method (a) and for the original MATHSM approach (b).

References:

[1] Elber, G.; Cohen, E.; Drake, S.: MATHSM: Medial Axis Transform toward High Speed Machining of Pockets. *Comput. Aided Design*, 37(2):241–250, Feb 2005. https://doi.org/10.1016/j.cad.2004.05.008.

[2] Held, M.: *On the Computational Geometry of Pocket Machining*, volume 500 of *Lecture Notes Comput. Sci.* Springer-Verlag, June 1991. ISBN 3-540-54103-9.

[3] Held, M.; Huber, S.: Topology-Oriented Incremental Computation of Voronoi Diagrams of Circular Arcs and Straight-Line Segments. *Comput. Aided Design*, 41(5):327–338, May 2009. https://doi.org/10.1016/j.cad.2008.08.004.

© 2024 U-turn Press LLC, http://www.cad-conference.net